Title
Conditional (intestinal-specific) knockout of the riboflavin transporter-3 (RFVT-3) impairs riboflavin absorption.

Journal
American journal of physiology. Gastrointestinal and liver physiology, 310(4)

ISSN
0193-1857

Authors
Subramanian, Veedamali S
Lambrecht, Nils
Lytle, Christian
et al.

Publication Date
2016-02-01

DOI
10.1152/ajpgi.00340.2015

Peer reviewed

Am J Physiol Gastrointest Liver Physiol 310: G285–G293, 2016.
First published December 10, 2015; doi:10.1152/ajpgi.00340.2015.

Conditional (intestinal-specific) knockout of the riboflavin transporter-3 (RFVT-3) impairs riboflavin absorption

Veedamali S. Subramanian,[1,2] Nils Lambrecht,[2] Christian Lytle,[3] and Hamid M. Said[1,2]

[1]*Departments of Medicine, Physiology and Biophysics, University of California, Irvine, California;* [2]*Department of Medical Research, Veterans Affairs Medical Center, Long Beach, California; and* [3]*Division of Biomedical Sciences, University of California, Riverside, California*

Submitted 28 September 2015; accepted in final form 2 December 2015

Subramanian VS, Lambrecht N, Lytle C, Said HM. Conditional (intestinal-specific) knockout of the riboflavin transporter-3 (RFVT-3) impairs riboflavin absorption. *Am J Physiol Gastrointest Liver Physiol* 310: G285–G293, 2016. First published December 10, 2015; doi:10.1152/ajpgi.00340.2015.—Riboflavin (RF) is indispensable for normal cell metabolism, proliferation, and growth. The RFVT-3 protein (product of the *Slc52a3* gene) is expressed in the gut with the expression being restricted to the apical membrane domain of the polarized intestinal epithelial cells. The relative contribution of RFVT-3 to total carrier-mediated RF uptake in the native intestine, however, is not clear. We addressed this issue in the current investigation using a conditional (intestinal-specific) RFVT-3 knockout (cKO) mouse model developed by the Cre/Lox approach. All RFVT-3 cKO mice were found to be RF deficient and showed a significant growth and development retardation; also, nearly two-thirds of them died prematurely between the age of 6 and 12 wk. In vivo (intestinal and colonic loops) and in vitro (native isolated intestinal epithelial cells) uptake studies showed a severe inhibition in carrier-mediated RF uptake in the cKO mice compared with control littermates. We also observed a significant increase in the level of expression of oxidative stress-responsive genes in the intestine of the cKO mice compared with control littermates. Supplementation of the RFVT-3 cKO mice with pharmacological doses of RF led to a complete correction of the growth retardation and to normalization in the level of expression of the oxidative stress-responsive genes in the gut. These results show, for the first time, that the RFVT-3 system is the main transporter involved in carrier-mediated RF uptake in the native mouse small and large intestine, and that its dysfunction impairs normal RF body homeostasis.

intestine

THE WATER-SOLUBLE VITAMIN riboflavin (RF) is required for normal cellular metabolism, proliferation, and growth. In the biologically active forms (flavin mononucleotide and flavin adenine dinucleotide), RF plays a key metabolic role in the transfer of electrons in biological oxidation-reduction reactions involving carbohydrate, lipid, amino acid, and certain water-soluble vitamins (pyridoxine and folate) (3, 32). Studies have also shown a role for RF in protein folding within the endoplasmic reticulum (38). More recent investigations have demonstrated anti-oxidant and anti-inflammatory properties for RF (13, 20, 33, 35), and further showed a role for the vitamin in normal immune function (23, 34). RF deficiency leads to a variety of abnormalities, including degenerative changes of the nervous system, anemia, skin lesions, cataract, and growth retardation (28, 32); RF deficiency also leads to an increase in the susceptibility to cancer (24). Deficiency/suboptimal levels of this micronutrient occur in chronic alcoholism, diabetes mellitus, inflammatory bowel disease, and Brown-Vialetto Van Laere and Fazio Londe syndromes [the latter are neurological disorders caused by mutations in RFVT-2 and -3 (1, 2, 4, 5, 9, 10, 14, 16, 17, 19, 29)].

Mammals cannot synthesize RF endogenously. Therefore, they must obtain the vitamin from exogenous sources via intestinal absorption. Two sources of RF are available to the intestine: a dietary source and a bacterial source [the latter is in regard to the vitamin produced by the microbiota of the large intestine (12, 15, 40)]. Previous studies from our laboratory and others have shown that small and large intestinal RF uptake is specific and carrier-mediated in nature (30–32). The recently cloned RF transporters-2 and -3 [RFVT-2 and -3; products of the *SLC52A2* and *SLC52A3* genes, respectively (6, 41, 42)] are both expressed in the gut, with expression of RFVT-3 being significantly higher than that of RFVT-2 (36, 42); the former is also more efficient in transporting RF than the latter (36). Also, live cell confocal imaging studies of polarized intestinal epithelial cells have shown that RFVT-3 is predominantly expressed at the apical membrane domain while RFVT-2 is mostly expressed at the basolateral membrane domain of these cells (36).

To date, however, the relative contribution of the RFVT-3 system to total carrier-mediated RF uptake in the native intestine in vivo is not well defined. Our recent in vitro study using the intestinal Caco-2 cell line and *SLC52A3* gene-specific small-interfering RNA approach showed an important role for RFVT-3 in RF uptake (36). The aim of this study was to define the role of RFVT-3 in RF uptake in native intestine in vivo, and for that we have generated a conditional (intestinal-specific) RFVT-3 cKO mouse model. Our results showed that the RFVT-3 system is indeed the main transporter involved in RF uptake in the native small and large intestine, and that dysfunction of this system negatively impacts RF body homeostasis.

MATERIALS AND METHODS

Materials

[^{3}H]RF and [^{3}H]biotin (specific activity 21.2 and 60 Ci/mmol, respectively; radiochemical purity >97% for both) were purchased from Moravek Biochemicals (Brea, CA) and American Radiolabeled Chemicals (St. Louis, MO), respectively. Anti-RFVT-3 polyclonal and anti-β-actin monoclonal antibodies were obtained from Gene Tex (Irvine, CA) and Santa Cruz Biotechnology (Santa Cruz, CA), respectively. Anti-rabbit IRDye-800 and anti-mouse IRDye-680 antibodies were purchased from LI-COR Bioscience (Lincoln, NE). All chemi-

Address for reprint requests and other correspondence: H. M. Said, UCI/VA Medical Program, VA Medical Center-151, Long Beach, CA 90822 (e-mail: hmsaid@uci.edu).

cals and reagents were purchased from commercial vendors and were of analytical/molecular biology grade.

Generation of Conditional (Intestinal-Specific) RFVT-3 cKO Mice

An 11.88-kb region of the *Slc52a3* gene was subcloned from a C57BL/6 BAC clone (RP23:424F10) using a homologous recombination-based technique (*inGenious* Targeting Laboratory, Ronkonkoma, NY). The region was designed such that the 5′-homology arm extends 6.55 kb to a single LoxP site. The 3′-homology arm extends 2.61 kb 3′ to a LoxP/FRT-flanked Neo cassette. A single LoxP site was inserted upstream of exon 2 in intron 1–2, and the LoxP/FRT-flanked Neo cassette was inserted downstream of exon 3 in intron 3–4. The size of the target region is 2.72 kb containing exons 2 and 3 (Fig. 1*A*).

Generation of the Homozygous LoxP$^{+/+}$ Mice

Identification of somatic Neo-deleted mice. Targeted iTL BA1 (129/SvEv × C57BL/6N) hybrid embryonic stem cells were microinjected in C57BL/6 blastocytes. Resulting chimeras with a high-percentage agouti coat color were mated to C57BL/6 FLP mice to remove the Neo cassette. The Neo deletion was confirmed by PCR using forward primer 5′-GTTGGTGATATGGTCTTCCAGATG-3′ and reverse primer 5′-CCAGGTGGGTCTGTGTTTGTAG-3′. Subsequently, a primer set (forward 5′-CACTGATATTGTAAGTAGTTTGC-3′ and reverse 5′-CTAGTGCGAAGTAGTGATCAGG-3′) was used to screen mice for presence of the FLP transgene. Additionally, a PCR was performed to detect the presence of the distal LoxP site using a forward primer 5′-TACTCTGTACAAGGAGGAGCCCTC-3′ and a reverse primer 5′-CAGATGATAACCTGGGAAAGATAGGG-3′. Finally, the 3′-homology arm integration was confirmed by PCR using forward primer 5′-TCACCAGGCTTCTTGTGTGTACAC-3′ and reverse primer 5′-GCATAAGCTTGGATCCGTTCTTCGGAC-3′.

Identification of germline Neo-deleted mice. The confirmed somatic Neo-deleted male mice were mated with C57BL/6N wild-type female mice to generate germline Neo-deleted mice. Resulting pups were genotyped for Neo deletion and confirmed heterozygote mice (*Slc52a3* LoxP$^{+/-}$) for germline Neo deletion and FLP absence.

Identification of homozygous germline neo-deleted mice. The confirmed germline Neo-deleted heterozygote mice (*Slc52a3* Lox$^{+/-}$) were mated to generate homozygous (*Slc52a3*) germline Neo-deleted mice. Resulting pups were genotyped for Neo deletion as described above and confirmed homozygote (*Slc52a3* LoxP$^{+/+}$).

The generated homozygous mice (*Slc53a3* LoxP$^{+/+}$) were mated with mice expressing intestinal specific Cre-recombinase (The Jackson Laboratory) under the control of the villin promoter. The villin gene is predominantly expressed in intestinal epithelial cells of the small bowel and the proximal portion of the large bowel (22). DNA isolated from ear samples of the offspring were genotyped for LoxP$^{+/+}$ sites and the presence of the Cre-recombinase using specific primers (for *Slc52a3* LoxP$^{+/+}$, the forward 5′-TACTCTGTACAAGGAGGAGCCCTC-3′ and the reverse 5′-GTTCACAGATAACCTTTAACT-3′; for Cre, the forward 5′-GTGTGGGACAGAGAACAAACC-3′ and the reverse 5′-ACATCTTCAGGTTCTGCGGG-3′). Deletion of exons 2 and 3 in the small bowel by villin promoter-driven Cre-recombinase expression was confirmed by PCR using intestinal mRNA. All breeding and animal studies were approved by the Long Beach Veterans Affairs Medical Center Institutional Animal Care and Use Committee.

[^{3}H]RF Uptake In Vivo by Jejunal/Colonic Loops, and In Vitro by Isolated Native Mouse Intestinal Epithelial Cells

Jejunal/colonic loops (~1 cm) were used for RF uptake experiments in vivo as described previously (7, 27). Briefly, the jejunal/colonic loops were filled with 100 μl of Krebs-Ringer (K-R) buffer (pH 7.4) containing [^{3}H]RF (or [^{3}H]biotin) with or without unlabeled 1 mM RF (or 1 mM biotin). Uptake measurement was performed after 5 min (39, 43) and expressed in femtomoles per milligram protein per 5 min.

Jejunal epithelial cells from adult (6–12 wk) cKO mice and their wild-type littermates were prepared for transport studies as described before (7, 27). Briefly, mice were killed by cervical dislocation, their jejunum was removed, and stool contents were washed out and then incubated in Hank's balanced salt solution supplemented with 0.5 mM DTT and 1.5 mM EDTA at 37°C water bath for 15 min. A suspension of enterocytes was transferred to 15-ml falcon tubes and centrifuged (1,500 *g* for 3 min), and the cells were resuspended in K-R buffer (pH 7.4). Enterocyte viability was checked by the Trypan blue exclusion method and found to be >87%. [^{3}H]RF uptake was determined by the rapid filtration method (11). Protein concentrations were determined using a Bio-Rad kit (Hercules, CA).

Quantitative RT-PCR

One microgram of total RNA was treated with DNase I, and cDNA was synthesized using an i-Script kit (Bio-Rad). RT-qPCR was performed using the CFX96 real-time i-Cycler (Bio-Rad) and SYBR green PCR kit (Bio-Rad). Primers used were specific for mouse RFVT-3 (forward 5′-GGATCAGTGGAAGCCAGTG-3′ and reverse 5′-GACCTGTTAGGCAGGAAGATG-3′) and mouse RFVT-2 (forward 5′-TGCTGGCCATCACCAA-3′ and reverse 5′-GCCAGAGACCTGCACA-3′). Additionally, RT-qPCR for stress-response genes glutathione peroxidase (GPX1, forward 5′-CTCTTTACCTTCCTGCGGAA-3′ and reverse 5′-GGACAGCAGGGTTTCTATGT-3′), superoxide dismutase (SOD1, forward 5′-GATGACTTGGGCAAAGGTGG-3′ and reverse 5′-CTGCGCAATCCCATCACTC-3′), and Flavin-containing monooxygenase 2 (FMO2, forward 5′-CAGTTTCAGACCACTGTCA-3′ and reverse 5′-TGTATTCGCGGCTATGGA-3′) was performed. The housekeeping gene used in all amplifications was mouse β-actin (forward 5′-ATCCTCTTCCTCCCTGGA-3′ and reverse 5′-TTCATGGATGCCACAGGA-3′). The relative expression was quantified by normalizing C_t values with corresponding β-actin as described before (21). The negative control reactions with respective gene-specific primers, PCR mix, and without RT product were used in every experiment.

Western Blot Analysis

Villus epithelial cells were isolated from the jejunum of RFVT-3 cKO mice and control littermates as described before (25). Cells were lysed in RIPA buffer (Sigma) containing complete protease inhibitor cocktail (Roche, NJ), and the soluble protein fraction was isolated by centrifugation at 12,000 revolutions/min for 10 min. SDS-PAGE of 60 μg of protein was performed on a 4–12% mini gel (Invitrogen). The protein was transferred to an immobilon polyvinylidene difluoride membrane, and the blot was blocked in LI-COR blocking buffer. The blot was simultaneously probed overnight with a mouse RFVT-3 antibody raised in rabbits along with a β-actin monoclonal antibody. The blot was washed three times in PBS-Tween 20 and then incubated with anti-rabbit IRDye 800 and anti-mouse IRDye 680 (LI-COR Bioscience) secondary antibodies (1:30,000) for 45 min at room temperature. The specific immunoreactive bands were captured using the Odyssey infrared imaging system (LI-COR Bioscience), and their densities were quantified using the LI-COR software (LI-COR Bioscience).

Measurement of Blood RF Levels

Blood levels of RF in the RFVT-3 cKO mice and sex-matched control littermates were determined using a glutathione reductase assay kit (Cayman Chemical, Ann Arbor, MI) (8). Briefly, blood samples were collected from dead mice, and the glutathione reductase activity was determined in erythrocytes as described in the manufacturer's protocol.

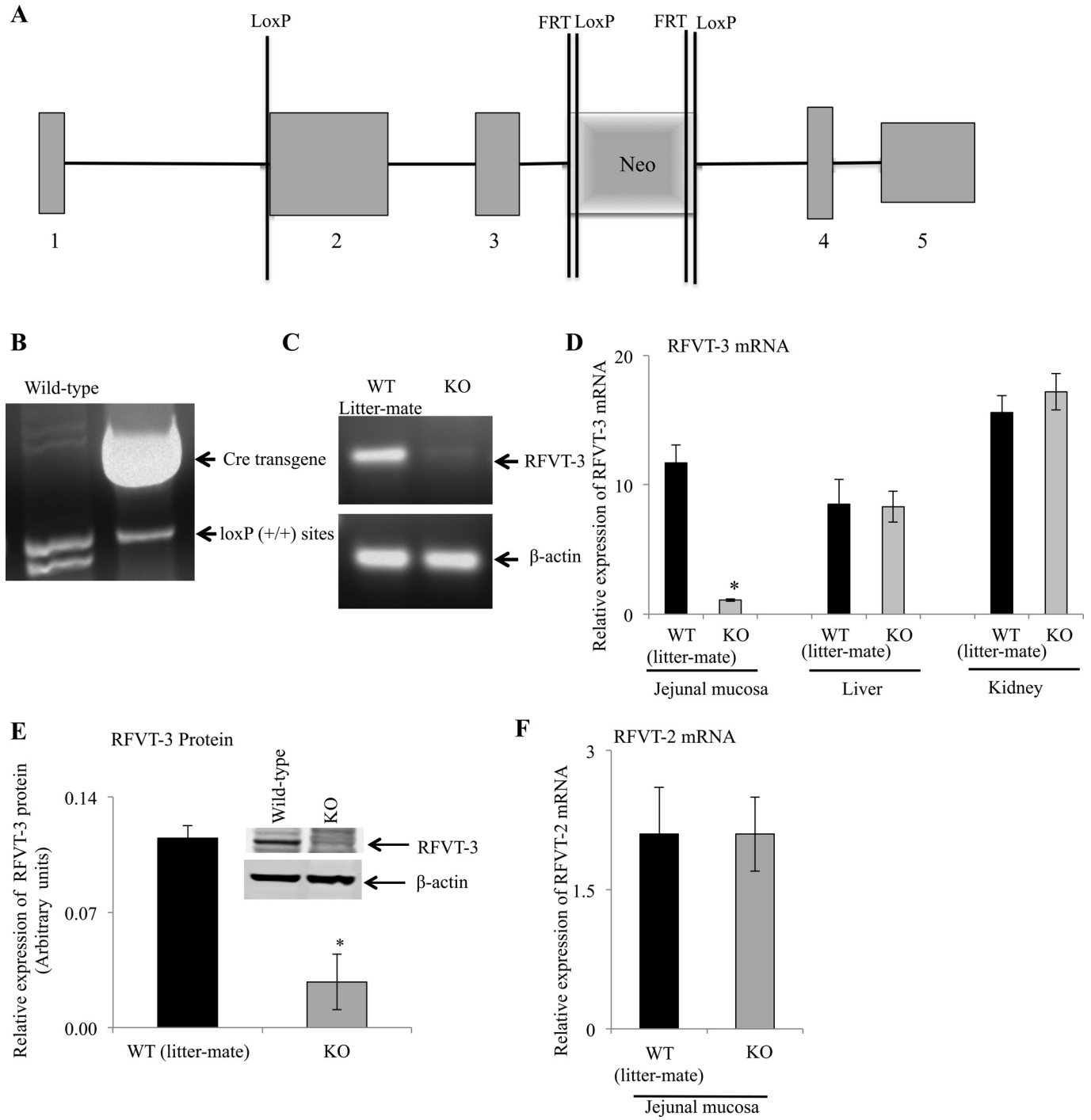

Fig. 1. Generation of conditional (intestinal-specific) RFVT-3 knockout (cKO) mice, genotyping, and validation of RFVT-3 loss at the protein and mRNA expression level. *A*: schematic depiction of the homologous recombination to introduce the LoxP site upstream of exon 2 and downstream of exon 3 of the *Slc52a3* gene. A 5′-LoxP recombination site was inserted in intron 1 of the *Slc52a3* gene together with a Neo cassette, and a second 3′-LoxP recombination site was introduced into intron 3. Exons 2 and 3 of the *Slc52a3* gene were crossed with transgenic mice expressing the Cre-recombinase in intestinal epithelial cells under the control of villin promoter. *B*: genomic PCR analysis of mouse ear DNA samples using two primer pairs to show the presence of $LoxP^{+/+}$ sites and Cre transgenes. *C*: loss of RFVT-3 mRNA expression due to conditional deletion of exons 2 and 3 of *Slc52a3* in the small intestine was confirmed by RT-qPCR. *D*: quantitative PCR from reverse-transcribed total RNA of jejunum mucosal scraping, liver and kidney of cKO mice, and their sex-matched littermates to determine the expression level of RFVT-3 as described in MATERIALS AND METHODS. Data are means ± SE of 6–9 sets of mice. $*P < 0.01$. *E*: expression of RFVT-3 protein in the intestine of the RFVT-3 cKO and control littermates. Western blot analysis was performed using specific anti-RFVT-3 polyclonal antibodies as described in MATERIALS AND METHODS. Data are means ± SE of at least 3 separate sets of mice. $*P < 0.01$. *F*: quantitative PCR from reverse-transcribed total RNA of jejunum mucosal scraping, liver and kidney of cKO mice, and their sex-matched littermates to determine the expression level of RFVT-2 as described in MATERIALS AND METHODS. Data are means ± SE of 6–9 sets of mice.

Phenotype Assessment

Body weight, bone density, and other changes were monitored in the RFVT-3 cKO mice and sex-matched wild-type littermates. Animals were anesthetized and placed in a Kodak Image station (Kodak Molecular Imaging Systems, New Haven, CT) for performing X-ray imaging analysis. Body weight was determined weekly using a Mettler Toledo scale. Estimation of bone density and determination of bone length in X-ray images were performed using Scion Image 4.0.3 (Scion, Frederick, MD).

Histology

The RFVT-3 cKO mice and sex-matched wild-type littermates were killed, and the intestine, heart, liver, and kidneys were immediately removed and fixed in 10% formalin overnight. The tissue samples were sectioned and paraffin embedded. Hematoxylin and eosin (H&E)-stained slides were prepared using standard histological techniques (Long Beach Veterans Medical Center Clinical Histology Laboratory). In another study the oriented histology section of the small bowel wall were semiquantitatively analyzed to measure the average villus height for each animal. Briefly, H&E-stained sections were viewed in a conventional Nikon Exclipse 50i microscope equipped with a ×10 ocular with a micrometer and a ×10 objective. The surface of the bowel mucosa was identified as the junction between crypts and villi, and the height of five representative villi was measured in five separate ×10 fields. The mean and SD were calculated. All groups of data were compared using the Student's *t*-test, and the difference of the mean with the SE was calculated. The microscopic analysis was performed by a board-certified anatomic pathologist.

Statistical Analysis

All data (uptake, RT-qPCR, and Western blot analysis) presented are means ± SE of at least three independent experiments with at least three different sets of animals. Uptake of [^{3}H]RF (and [^{3}H]biotin) by the carrier-mediated process was determined by subtracting uptake in the presence of 1 mM of unlabeled RF (or biotin) from that in its absence. In all studies, simultaneously performed controls (sex-matched littermates) were used. The statistical significance was set at $P < 0.05$ and was calculated using the Student's *t*-test.

RESULTS

Generation and Establishment of the Conditional (Intestinal-Specific) RFVT-3 cKO Mouse Colony

Recent studies from our laboratory and others have shown that the RFVT-3 is expressed in the gut and that the expression is restricted to the apical membrane domain of intestinal epithelial cells (36). The contribution of RFVT-3 to total carrier-mediated RF uptake by the native intestine, however, is not known. The mouse is a good animal model to study intestinal RF transport physiology because the murine intestine shares a similar intestinal RF uptake process with humans. Moreover, murine RFVT-3 shares a high degree of sequence homology with the human RFVT-3 (www.Genome.jp/tools/clustlw). Accordingly, we chose this animal to develop a RFVT-3 cKO model and used the cKO mouse to study intestinal RF uptake in vivo. A homozygous mouse (*Slc52a3* LoxP$^{+/+}$) was generated (*inGenious* Targeting Laboratory) (Fig. 1*A*) and bred with a mouse that expresses the intestinal-specific Cre-recombinase under the control of the villin promoter to obtain an intestinal-specific RFVT-3 cKO mouse. Figure 1*B* shows the presence of Cre-recombinase and LoxP$^{+/+}$ sites in the offspring. We confirmed the intestinal-specific deletion of the *Slc52a3* gene at both the mRNA (PCR) in the gut [and its normal expression in other tissues (liver and kidney)] (Fig. 1, *C* and *D*) and the protein (Western blotting) levels (Fig. 1*E*). Finally, we did not observe any change in the level of expression of the other RF transporter that is also expressed in the gut, i.e., the RFVT-2, in the intestine of the RFVT-3 cKO mice (Fig. 1*F*). These findings confirm the intestinal-specific nature of the RFVT-3 cKO and shows that such a knockout does not lead to an induction in the level of expression of RFVT-2 in the gut.

Phenotype Assessment of the RFVT-3 cKO Mice

The phenotype of the RFVT-3 cKO mice showed a remarkable difference compared with sex-matched wild-type littermates (Fig. 2). All RFVT-3 cKO mice showed significant growth retardation, and nearly two-thirds of them died prematurely between the age of 6 and 12 wk. Also, the cKO animals exhibited lethargic behavior, hunched back posture, and ocular surface abnormalities compared with wild-type littermates (Fig. 2, *A* and *B*). Total body weight of the RFVT-3 cKO animals was significantly ($P < 0.01$) lower than that of age- and sex-matched wild-type littermates (Fig. 2*C*). In addition, X-ray image analysis of RFVT-3 cKO mice compared with wild-type littermates showed a significant ($P < 0.001$) decrease in bone density (femur and tibia; Fig. 2*D*) and a significantly ($P < 0.001$) shorter femur, tibial, and pelvic bones (Fig. 2*E*). However, no histological abnormalities were found in the heart, liver, kidney, jejunum, ileum, cecum, and proximal and distal colon of the RFVT-3 cKO mice (data not shown). In addition, no significant changes in the length of the jejunal crypts and villi of the cKO mice compared with control littermates were seen (data not shown). Finally, a significantly ($P < 0.01$) lower RF blood level (erythrocyte glutathione reductase activity was measured to reflect the level of RF in blood samples; see MATERIALS AND METHODS) was found in the RFVT-3 cKO mice compared with their sex-matched littermate controls (Fig. 2*F*).

Effect of Loss of RFVT-3 on Intestinal RF Uptake

We used both an in vivo (gut loops) and an in vitro (isolated intestinal epithelial cells) preparation to examine the effect of knocking out the intestinal RFVT-3 on gut RF uptake. Results were compared with RF uptake by the same preparation from sex-matched littermate controls. The results showed RF (0.24 μM) uptake to be severely ($P < 0.01$) inhibited in jejunal loops of RFVT-3 cKO mice compared with control littermates (Fig. 3*A*). No such inhibition was observed in the uptake of the unrelated vitamin biotin (83 nM) by jejunal loop of RFVT-3 cKO mice compared with uptake by their control littermates (Fig. 3*B*). The latter finding confirms specificity of the RFVT-3 cKO model. Similarly, RF uptake by epithelial cells freshly isolated from the jejunum of RFVT-3 cKO mice was found to be significantly ($P < 0.01$) suppressed compared with uptake by cells from control littermates (Fig. 3*C*) [the residual RF uptake observed in this preparation from the RFVT-3 cKO mice is most likely due to uptake across the exposed basolateral membrane where RFVT-2 is expressed (36)].

Previous studies have shown that the normal microflora of the large intestine synthesizes a considerable amount of RF (12, 15, 40) and that colonocytes have an efficient carrier-

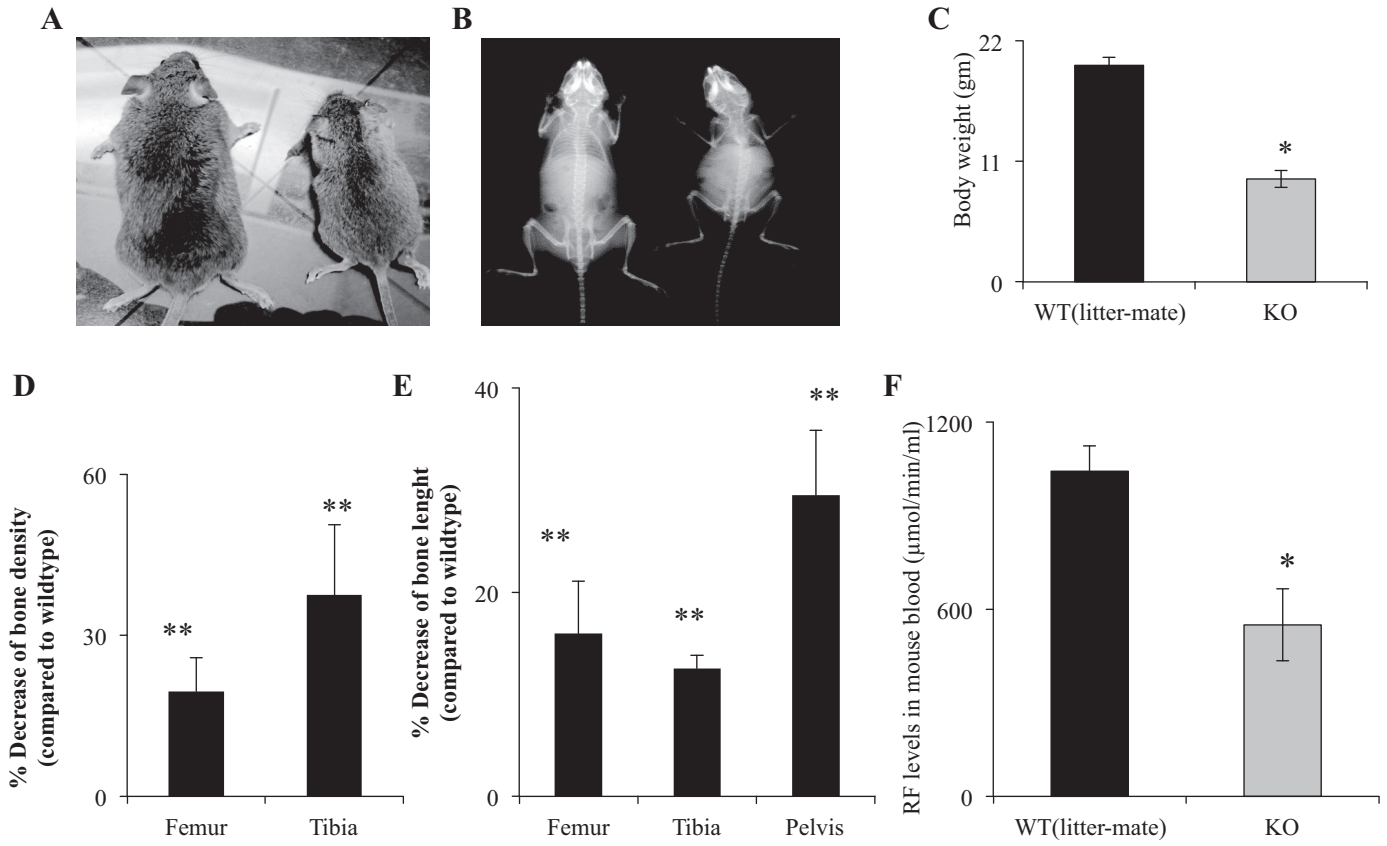

Fig. 2. Effect of the RFVT-3 cKO on mouse phenotype (body weight and bone density and length) and riboflavin (RF) blood level. *A*: representative image of a cKO mouse (*right*) and sex-matched wild-type littermate (*left*) showing ~50% reduction in their body size. *B*: representative X-ray image of a cKO mouse (*right*) and sex-matched wild-type littermate (*left*) showing difference in size and bone length. *C*: bar graph showing marked difference in body weight of cKO mice compared with control littermates (*$P < 0.01$). *D*: bar graph showing significant decrease in bone density in cKO mice (expressed as %relative to wild-type littermates) (**$P < 0.001$). *E*: bar graph showing significant decrease in bone length in cKO mice (expressed as %relative to wild-type littermates) (**$P < 0.001$). *F*: RF levels in blood of cKO mice and wild-type littermates. *$P < 0.01$. Data are means ± SE of 6 sets of mice.

mediated mechanism for RF uptake (37). Therefore, we also examined carrier-mediated RF (0.24 μM) uptake in vivo in the colon of the RFVT-3 cKO mice and compared it with uptake with control littermates. The results again showed a significant ($P < 0.01$) inhibition in carrier-mediated RF uptake in the colon of RFVT-3 cKO mice compared with sex-matched control littermates (Fig. 4*A*). The residual expression of RFVT-3 in the colon (Fig. 4*B*) is likely due to the fact that the villin expression decreases in the distal portion of the colon (22), which leads to a decrease in Cre expression and thus less

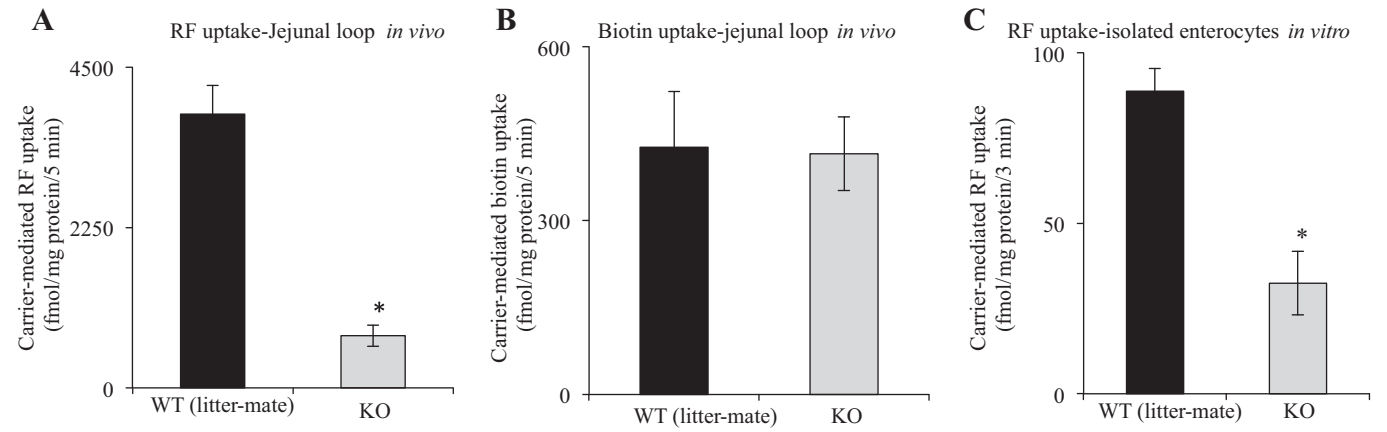

Fig. 3. Determination of effect and specificity of the RFVT-3 cKO on RF uptake in vivo and in vitro. *A*: carrier-mediated RF uptake by in vivo jejunal loop of cKO mice and sex-matched littermates. B: carrier-mediated biotin uptake by in vivo jejunal loop of RFVT-3 cKO mice and control littermates. *C*: carrier-mediated RF uptake by in vitro freshly isolated intestinal epithelial cells of cKO mice and wild-type littermates. Data are means ± SE of at least 3 separate uptake determinations performed on at least 3 different sets of mice. *$P < 0.01$.

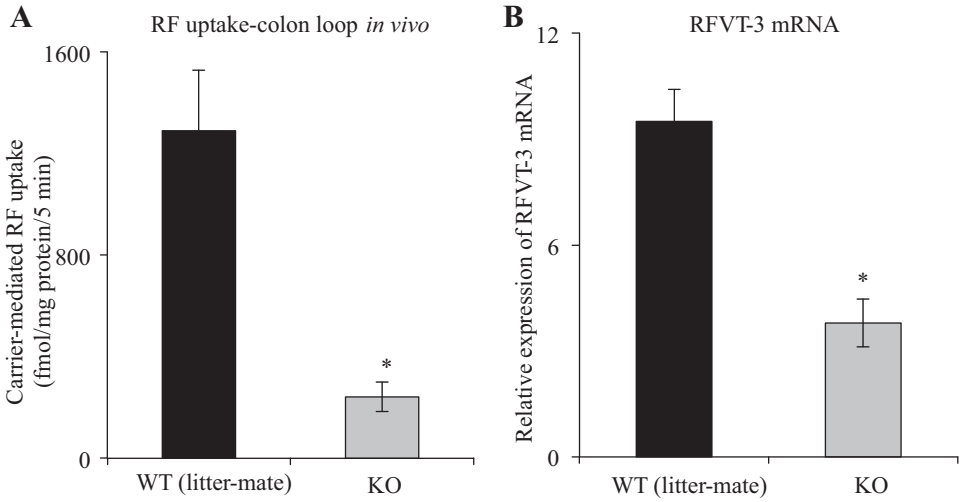

Fig. 4. Effect of the RFVT-3 cKO on carrier-mediated RF uptake in the colon, and on the level of mRNA expression of RFVT-3. *A*: carrier-mediated RF uptake by in vivo intact colonic loop of cKO mice and their sex-matched littermates. *B*: quantitative PCR from reverse-transcribed total RNA of colon of cKO mice and their sex-matched littermates was performed to determine the expression level of RFVT-3. Data are means ± SE of 4 different determinations from 4 different sets of mice. $*P < 0.01$.

efficient RFVT-3 gene knockout in that part of the colon (22). No change in level of expression of the RFVT-2 mRNA was found in the colon of RFVT-3 cKO compared with control littermates (2.6 ± 1 and 3.1 ± 0.6 arbitrary units in wild-type littermates and cKO, respectively,).

Level of Expression of Oxidative Stress-Responsive Genes in the Intestine of the RFVT-3 cKO Mice

Recent studies have shown that RF deficiency leads to oxidative stress in intestinal epithelial cells (18). Therefore, we examined the effect of loss of RFVT-3 expression in the intestine on level of expression of oxidative stress-responsive genes (FMO2, GPX1, and SOD1) in the jejunum; results were compared with those obtained with control littermates. The results showed a significant ($P < 0.01$ for all) increase in the level of mRNA expression of FMO2, GPX1, and SOD1 in jejunal mucosa of RFVT-3 cKO compared with wild-type littermates (Fig. 5, *A–C*, respectively). These findings are in line with a state of depletion of RF in intestinal epithelial cells and points to a role for RF in the maintenance of normal intestinal health (18, 26).

Effect of RF Supplementation of the RFVT-3 cKO Mice on Animal Phenotype

In this study, we examined the effect of supplementing the RFVT-3 KO mice with pharmacological amounts of RF on the observed growth retardation, changes in bone density and length, and on the ocular surface abnormalities and early death phenotypes. This was done by providing RF (500 μM) in the drinking water to dams during pregnancy and lactation, and to the RFVT-3 cKO mice throughout their life. The results showed that RF supplementation of the RFVT-3 cKO mice led to correction of all the above-described abnormal phenotypes and that the KO animals grew at a similar rate as their control littermates (Fig. 6, *A* and *B*). In addition, the level of expression of the oxidative stress-responsive genes (FMO2, GPX1, and SOD1) was found to be similar in the jejunum of the RFVT-3 cKO mice and wild-type littermates (Fig. 6, *C–E*, respectively).

DISCUSSION

The aim of this study was to develop a better understanding of the role of the recently cloned RFVT-3 in the intestinal carrier-mediated absorption process of RF in the native gut in vivo. RF, a member of the B family of water-soluble vitamins, plays critical roles in normal cellular metabolism and function of humans and other mammals. However, it cannot be synthesized endogenously and, thus, must be obtained from exogenous sources via intestinal absorption. To achieve our aim, we developed a RFVT-3 cKO mouse model using the Cre/Lox approach and verified the near absence of the RFVT-3 protein/mRNA in the gut of the cKO animals compared with their sex-matched wild-type littermates. We also showed that ex-

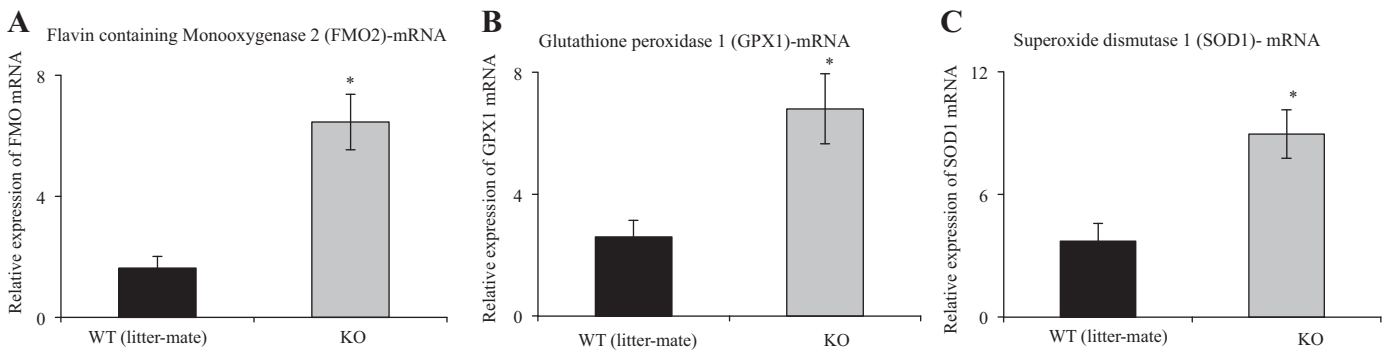

Fig. 5. Effect of the RFVT-3 cKO on level of mRNA expression of oxidative stress response genes. Quantitative PCR from reverse-transcribed total RNA of jejunum mucosal scraping was used to determine the mRNA expression level of flavin-containing monooxygenase 2 (FMO2, *A*), glutathione peroxidase (GPX1, *B*), and superoxide dismutase (SOD1, *C*). Data are means ± SE of 4 different sets of mice. $*P < 0.01$.

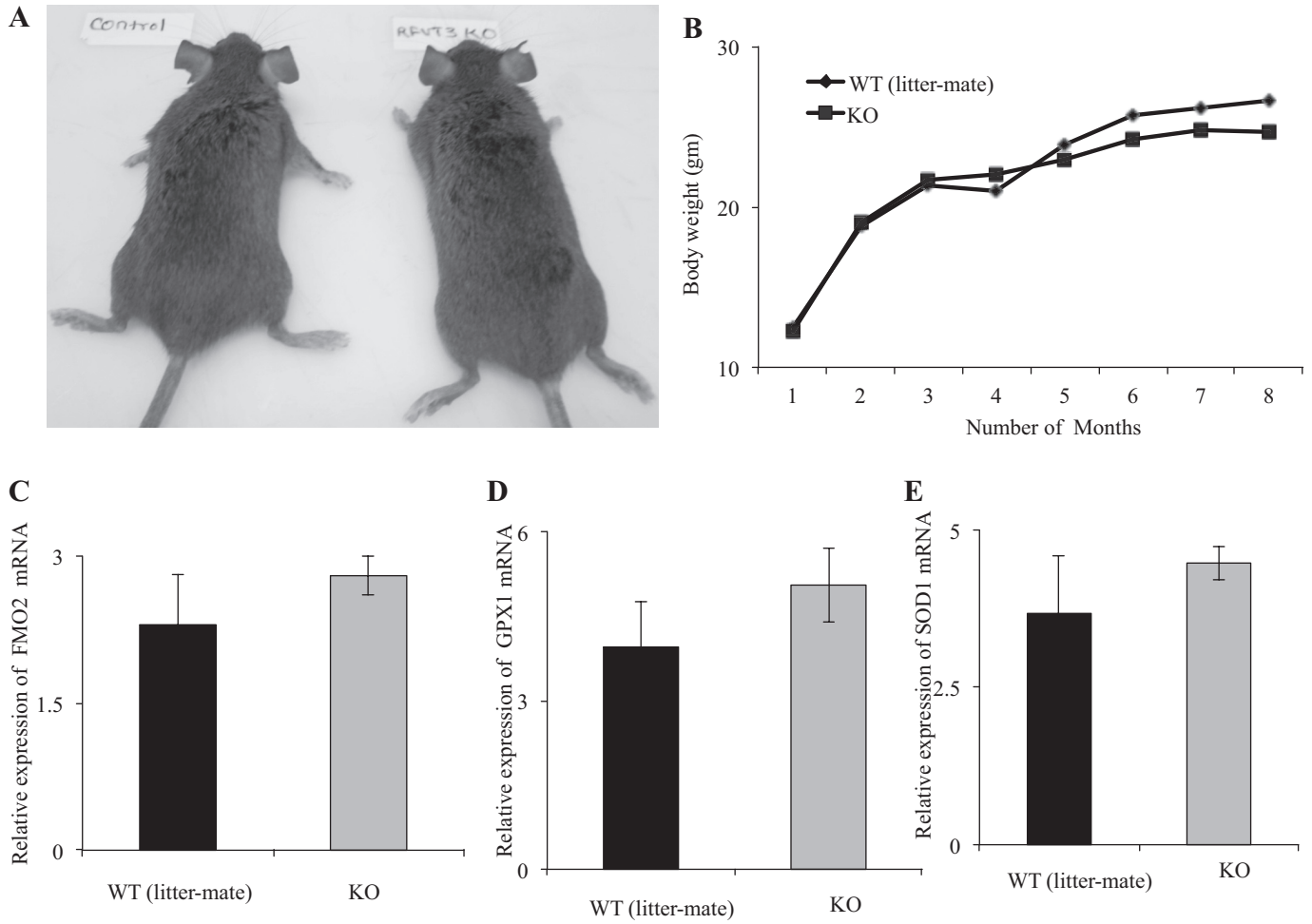

Fig. 6. Effect of RF supplementation of the RFVT-3 cKO mice on their observed phenotype. *A*: representative image of a RFVT-3 cKO mouse (*right*) and sex-matched control littermate (*left*) showing similar body size. *B*: graph showing similar body weight of cKO mice compared with wild-type littermates. *C*}*E*: quantitative PCR from reverse-transcribed total RNA of jejunum mucosal scraping was used to determine the level of mRNA expression of FMO2 (*C*), GPX1 (*D*), and SOD1 (*E*). Data are means ± SE of 4 different sets of mice.

pression of RFVT-3 in other tissues (liver and kidney) is not affected, i.e., similar in the cKO animals and their control littermates. Furthermore, we found that knocking out the RFVT-3 system in the intestine does not lead to induction in the expression of RFVT-2, an RF transporter that is also expressed in the gut.

Our results showed that all RFVT-3 cKO mice develop distinct phenotypes that include growth retardation (total body weight was markedly decreased compared with control littermates), decreased bone density and length, lethargic behavior, hunched back posture, and ocular surface abnormalities compared with wild-type littermates. In addition, their blood RF level was found to be significantly lower than that of control littermates, pointing to an important role for the RFVT-3 system in the maintenance of normal RF body homeostasis. Finally, almost two-thirds of the RFVT-3 cKO mice died prematurely between the age of 6 and 12 wk. The cause of death is not clear but could not be attributed to histological abnormalities in critical organs of the RFVT-3 cKO mice, since no such abnormalities were observed in the heart, liver, kidney, and the small and large intestine.

Our transport investigations in the native small intestine (jejunum) of the RFVT-3 cKO mice in vivo showed severe inhibition in carrier-mediated RF uptake compared with uptake by the jejunum of the wild-type littermates. In contrast, uptake of the unrelated vitamin biotin was found to be similar in the RFVT-3 cKO mice and to control littermates demonstrating substrate specificity of the knockout. Likewise, RF uptake in freshly isolated native jejunal epithelial cells in vitro was severely inhibited in the RFVT-3 cKO mice compared with control littermates. Similarly, carrier-mediated RF uptake in the native colon in vivo was found to be severely reduced in the RFVT-3 cKO mice compared with uptake in the colon of wild-type littermates. These findings clearly show that RFVT-3 plays an important role in the absorption of both dietary RF (which takes places in the small intestine) and the microbiota-generated RF (which takes place in the large intestine).

Recent studies have shown that RF deficiency leads to oxidative stress in intestinal epithelial cells (18, 26). Thus, we investigated the effect of loss of RFVT-3 expression in the intestine on level of expression of the oxidative stress-responsive genes FMO2, GPX1, and SOD1. Our results showed the expression of all these genes to be markedly increased in the jejunal mucosa of the RFVT-3 cKO mice compared with wild-type littermates. These data support an important role of RF in maintenance of normal intestinal health (18, 26).

Finally, the results of the effect of RF supplementation [RF (500 μM) was added to the drinking water of dams during pregnancy and lactation, and to the cKO mice during their entire life span] of the RFVT-3 cKO mice showing reversal of all observed abnormal phenotypes (growth retardation, bone density and length, ocular surface abnormalities, and early death) as well as the restoration in the level of expression of oxidative stress-responsive genes clearly demonstrate the importance of RF in overall health, growth, and development.

In summary, results of these investigations provide clear evidence for the essential role played by RFVT-3 in carrier-mediated RF uptake in native intestine in vivo, and in the maintenance of normal RF body homeostasis. It is hoped that the development of this mouse model, which allows the generation of tissue-specific deletion of RFVT-3, would serve as a catalyst for further investigations into the role of this recently identified and important RF transporter in the physiology/pathophysiology of other critical tissues.

GRANTS

This work was supported by grants from the Department of Veterans Affairs and the National Institutes of Health (DK-58057 and DK-56061).

DISCLOSURES

No conflicts of interest, financial or otherwise, are declared by the authors.

AUTHOR CONTRIBUTIONS

V.S.S., N.L., and H.M.S. conception and design of research; V.S.S., N.L., and C.L. performed experiments; V.S.S., N.L., and H.M.S. analyzed data; V.S.S., N.L., C.L., and H.M.S. interpreted results of experiments; V.S.S. and N.L. prepared figures; V.S.S. and H.M.S. drafted manuscript; V.S.S., N.L., C.L., and H.M.S. edited and revised manuscript; V.S.S., N.L., and H.M.S. approved final version of manuscript.

REFERENCES

1. **Bonjour JP.** Vitamins and alcoholism. V Riboflavin, VI Niacin, VII Pantothenic acid, and VIII Biotin. *Int J Vitam Nutr Res* 50: 425–440, 1980.
2. **Bosch AM, Abeling NG, Ijlst L, Knoester H, van der Pol Wl, , Stroomer AE, Wanders RJ, Visser G, Wijburg FA, Duran M, Waterham HR.** Brown-Vialetto-Van Laere and Fazio Londe syndrome is associated with a riboflavin transporter defect mimicking mild MADD: a new inborn error of metabolism with potential treatment. *J Inherit Metab Dis* 34: 159–164 2011.
3. **Cooperman JM, Lopez R.** Riboflavin. In: *Handbook of Vitamins: Nutritional, Biochemical and Clinical Aspects*, edited by Machlin LJ. New York, NY: Dekker, 1984, p. 299–327.
4. **Fennelly J, Frank O, Baker H, Leevy CM.** Peripheral neuropathy of the alcoholic. I. Aetiological role of aneurin and other B-complex vitamins. *Br Med J* 2: 1290–1292, 1965.
5. **Fernandez-Banares F, Abad-Lacruz A, Xiol X, Gine JJ, Dolz C, Cabre E, Esteve M, Gonzalez-Huix F, Gassull MA.** Vitamin status in patients with inflammatory bowel disease. *Am J Gastroenterol* 84: 744–48, 1989.
6. **Fujimura M, Yamamoto S, Murata T, Yasujima T, Inoue K, Ohta KY, Yuasa H.** Functional characteristics of the human ortholog of riboflavin transporter 2 and riboflavin-responsive expression of its rat ortholog in the small intestine indicate its involvement in riboflavin absorption. *J Nutr* 140: 1722–1727, 2010.
7. **Ghosal A, Lambrecht N, Subramanya SB, Kapadia Said HM.** Conditional knockout of the *Slc5a6* gene in mouse intestine impairs biotin absorption. *Am J Physiol Gastrointest Liver Physiol* 304: G64–G71, 2013.
8. **Graham JM, Peerson JM, Haskell MJ, Shrestha RK, Brown KH, Allen LH.** Erythrocyte riboflavin for the detection of Riboflavin deficiency in pregnant Nepali Women. *Clin Chem* 51: 2162–2165, 2005.
9. **Green P, Wiseman M, Crow YJ, Houlden H, Riphagen S, Lin JP, Raymond FL, Childs AM, Sheridan E, Edwards S, Josifova DJ.** Brown-Vialetto-Van Laere syndrome, a ponto-bulbar palsy with deafness, is caused by mutations in c20orf54. *Am J Hum Genet* 86: 485–89, 2010.
10. **Ho G, Yonezawa A, Masuda S, Inui K, Sim KG, Carpenter K, Olsen RK, Mitchell JJ, Rhead WJ, Peters G, Christodoulou J.** Maternal riboflavin deficiency, resulting in transient neonatal-onset glutaric aciduria type 2, is caused by a microdeletion in the riboflavin transporter gene GPR172B. *Hum Mutat* 32: E1976–E1984, 2011.
11. **Hopfer U, Nelson K, Perrotto J, Isselbacher KJ.** Glucose transport in isolated brush border membrane from rat small intestine. *J Biol Chem* 248: 25–32, 1973.
12. **Iinuma S.** Synthesis of riboflavin by intestinal bacteria. *J Vitaminol (Kyoto)* 1: 6–13, 1955.
13. **Iwanaga K, Hasegawa T, Hultquist DE, Harada H, Yoshikawa Y, Yanamadala S, Liao H, Visovatti SH, Pinsky DJ.** Riboflavin-mediated reduction of oxidant injury, rejection, and vasculopathy after cardiac allotransplantation. *Transplant* 83: 747–753, 2007.
14. **Johnson JO, Gibbs JR, Megarbane A, Urtizberea JA, Hernandez DG, Foley AR, Arepalli S, Pandraud A, Simon-Sanchez J, Clayton P, Reilly MM, Muntoni F, Abramzon Y, Houlden H, Singleton AB.** Exome sequencing reveals riboflavin transporter mutations as a cause of motor neuron disease. *Brain* 135: 2875–2882, 2012.
15. **Kasper H.** Vitamin absorption in the colon. *Am J Proctol* 21: 341–345, 1970.
16. **Kodentsova VM, Vrzhesinskaia OA, Trofimenko EV, Sokonikov AA, Beketova NA, Blazheevich NV, Isaeva VA, Aleinik SI, Trofimenko LS, Dronova VI.** [Vitamin status of children with diabetes mellitus]. *Vopr Med Khim* 40: 45–8, 1994.
17. **Kuroki F, Iida M, Tominaga M, Matsumoto T, Hirakawa K, Sugiyama S, Fujishima M.** Multiple vitamin status in crohn's disease: correlation with disease activity. *Dig Dis Sci* 38: 1614–1618, 1993.
18. **Lee ES, Corfe BM, Powers HJ.** Riboflavin depletion of intestinal cells in vitro leads to impaired energy generation and enhanced oxidative stress. *Eur J Nutr* 52: 1513–1521, 2013.
19. **Leevy CM, Baker H.** Vitamins and alcoholism. Introduction. *Am J Clin Nutr* 21: 1325–1328, 1968.
20. **Liu D, Zempleni J.** Low activity of LSD1 elicits a pro-inflammatory gene expression profile in riboflavin-deficient human T Lymphoma Jurkat cells. *Genes Nutr* 9: 422, 2014.
21. **Livek KJ, Schmittgen TD.** Analysis of relative gene expression data using real-time quantitative PCR and the 2(-delta DeltaC(T)) method. *Methods* 25: 402–408, 2001.
22. **Madison BB, Dunbar L, Qiao XT, Braunstein E, Gumucio DL.** Cis elements of the villin gene control expression in restricted domains of the vertical (crypt) and horizontal (duodenum, cecum) axes of the intestine. *J Biol Chem* 277: 33275–33283, 2002.
23. **Mazur-Bialy AI, Buchala B, Plytycz B.** Riboflavin deprivation inhibits macrophage viability and activity - a study on the RAW 264.7 cell line. *Br J Nutr* 110: 509–514, 2013.
24. **Pangrekar J, Krishnaswamy K, Jagadeesan V.** Effects of riboflavin deficiency and riboflavin administration on carcinogen-DNA binding. *Food Chem Toxicol* 31: 745–750, 1993.
25. **Pinkus LM.** Separation and use of enterocytes. *Methods Enzymol* 77: 154–162, 1981.
26. **Powers HJ.** Riboflavin (vitamin B2), health. *Am J Clin Nutr* 77: 1352–1360, 2003.
27. **Reidling JC, Lambrecht N, Kassir M, Said HM.** Impaired intestinal vitamin B1 (thiamin) uptake in thiamin transporter-2-deficient mice. *Gastroenterology* 138: 1802–1809, 2010.
28. **Rivilin RS.** Riboflavin. In: *Encyclopedia of Dietary Supplements*, edited by Coates PM, Betz JM, and Blackman MR. London, UK: Informa Healthcare, 2010, p. 691–699.
29. **Rosenthal WS, Adham NF, Lopez R, Cooperman JM.** Riboflavin deficiency in complicated chronic alcoholism. *Am J Clin Nutr* 26: 858–860, 1973.
30. **Said HM, Arianas P.** Transport of riboflavin in human intestinal brush border membrane vesicles. *Gastroenterology* 100: 82–88, 1990.
31. **Said HM, Hollander D, Mohammadkhani R.** Uptake of riboflavin by intestinal basolateral membrane vesicles: a specialized carrier-mediated process. *Biochim Biophys Acta* 1148: 263–268, 1993.

32. **Said HM, Ross C.** Riboflavin. In: *Modern Nutrition in Health and Disease Modern Nutrition in Health and Disease* (11th ed.), edited by Ross C, Caballero B, Cousins RJ, Tucker KL, Ziegler TR. p. 325–330, 2011.
33. **Sanches SC, Ramalho LN, Mendes-Bras M, Terra VA, Cecchini R, Augusto MJ, Ramalho FS.** Riboflavin (vitamin B-2) reduces hepatocellular injury following liver ischaemia and reperfusion in mice. *Food Chem Toxicol* 67: 65–67, 2014.
34. **Schramm M, Wiegmann K, Schramm S, Gluschko A, Herb M, Utermohlen O, Kronke M.** Riboflavin (vitamin B2) deficiency impairs NADPH oxidase 2 (Nox2) priming and defense against Listeria monocytogenes. *Eur J Immunol* 44: 728–741, 2014.
35. **Seekamp A, Hultquist DE, Till GO.** Protection by vitamin B2 against oxidant-mediated acute lung injury. *Inflamm* 23: 449–460, 1999.
36. **Subramanian VS, Subramanya SB, Rapp L, Marchant JS, Ma TY, Said HM.** Differential expression of human riboflavin transporters-1, -2, and -3 in polarized epithelia: a key role for hRFT-2 in intestinal riboflavin uptake. *Biochim Biophys Acta* 1808: 3016–3021, 2011.
37. **Tomie S, Yuasa H, Inoue K, Watanabe J.** Transport functions of riboflavin carriers in the rat small intestine and colon: site difference and effects of tricyclic-type drugs. *Drug Deliv* 8: 119–124, 2001.
38. **Tu BP, Ho-Schleyer SC, Travers KJ, Weissman JS.** Biochemical basis of oxidative protein folding in the endoplasmic reticulum. *Science* 290: 1571–1574, 2000.
39. **Vaziri ND, Said HM, Hollander D, Barbari A, Patel N, Dang D, Kariger R.** Impaired intestinal absorption of riboflavin in experimental uremia. *Nephron* 41: 26–29, 1985.
40. **Wrong OM, Edmonds CJ, Chadwich VS.** Vitamins. In: *The Large Intestine; Its Role In mammalian Nutrition and Homeostasis*. New York, NY: Wiley, p. 157–166, 1981.
41. **Yamamoto S, Inoue K, Ohta KY, Fukatsu R, Maeda JY, Yoshida Y, Yuasa H.** Identification and functional characterization of rat riboflavin transporter 2. *J Biochem* 145: 437–443, 2009.
42. **Yao Y, Yonezawa A, Yoshimatsu H, Masuda S, Katsura T, Inui K.** Identification and comparative functional characterization of a new human riboflavin transporter hRFT3 expressed in the brain. *J Nutr* 140: 1220–1226, 2010.
43. **Yoshimatsu H, Yonezawa A, Yao Y, Sugano K, Nakagawa S, Omura T, Matsubara K.** Functional involvement of RFVT3/SLC52A3 in intestinal riboflavin absorption. *Am J Physiol Gastrointest Liver Physiol* 306: G102–G110, 2014.